Shell-model Study of Nuclear Weak Rates and Astrophysical Applications

Toshio Suzuki

Nihon University, Tokyo

CANHP 2015, Kyoto

Sept. 30, 2015

○ New shell-model Hamiltonians

SFO (p-shell), GXPF1J (fp-shell), USDB (sd-shell)

Spin modes -GT strengths, M1 moments- are well described.

→ Accurate evaluation of spin-dependent transition rates

○ ν-nucleus reactions

- ν-^{12}C, ν-^{56}Fe reactions with SFO and GXPF1J
- Nucleosynthesis of light elements, ^{7}Li and ^{11}B, (and ^{55}Mn) in supernova explosions (SNe)

  ν oscillations effects and ν oscillation parameters

○ e-capture and β-decay rates in stellar environments

- e-capture rates in pf-shell nuclei with GXPF1J

  Type-Ia supernova explosions and nucleosynthesis
- e-capture and β-decay rates in sd-shell nuclei and cooling of stars by URCA processes
- β-decay half-lives of waiting-point nuclei at N=126 and r-process nucleosynthesis

○New shell-model Hamiltonians and successful description of Gamow-Teller (GT) strengths

SFO (p-shell): GT in ^{12}C, ^{14}C

Suzuki, Fujimoto, Otsuka, PR C69, (2003)

GXPF1J (fp-shell): GT in Fe and Ni isotopes, M1 strengths

Honma, Otsuka, Mizusaki, Brown, PR C65 (2002); C69 (2004)

Suzuki, Honma et al., PR C79, (2009)

VMU (monopole-based universal interaction)

Otsuka, Suzuki, Honma, Utsuno et al., PRL 104 (2010) 012501

* important roles of tensor force

Monopole terms of V_{NN}

$$V_M^T(j_1 j_2) = \frac{\sum_J (2J+1) < j_1 j_2; JT | V | j_1 j_2; JT >}{\sum_J (2J+1)}$$

$j_> - j_<$: attractive

$j_> - j_>, j_< - j_<$: repulsive

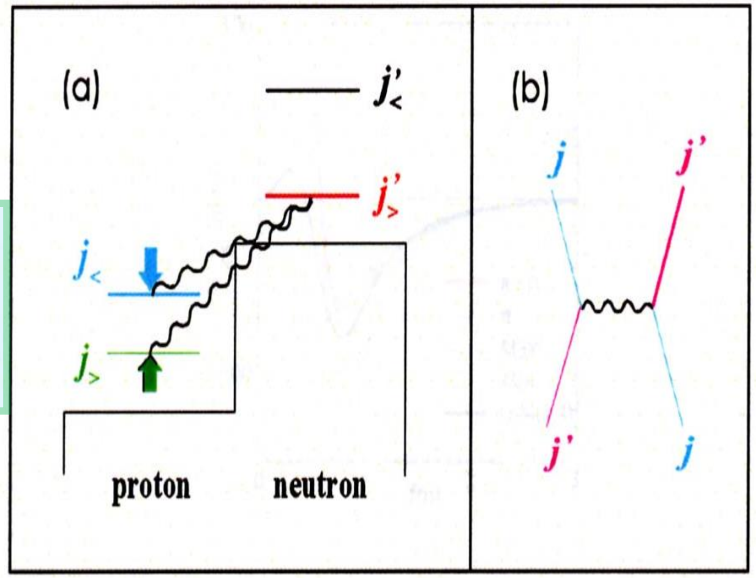

Otsuka, Suzuki, Fujimoto, Grawe, Akaishi, PRL 69 (2005)

Monopole terms: New SM interactions vs. microscopic G matrix

tensor force

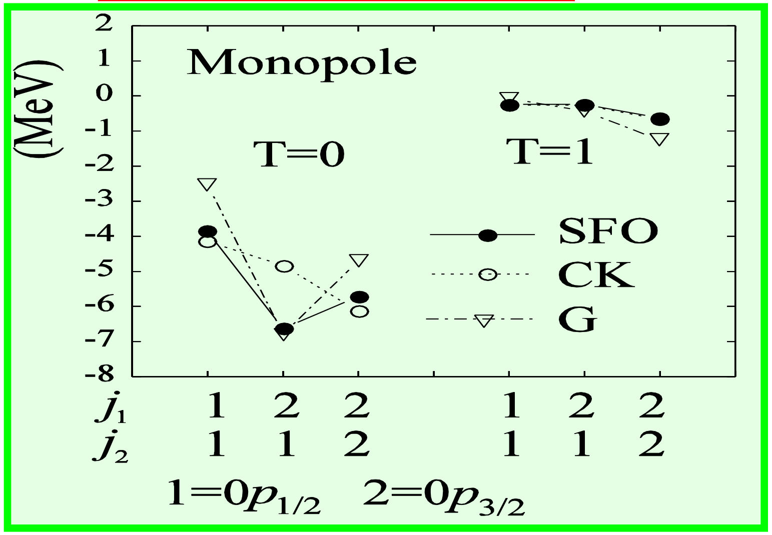

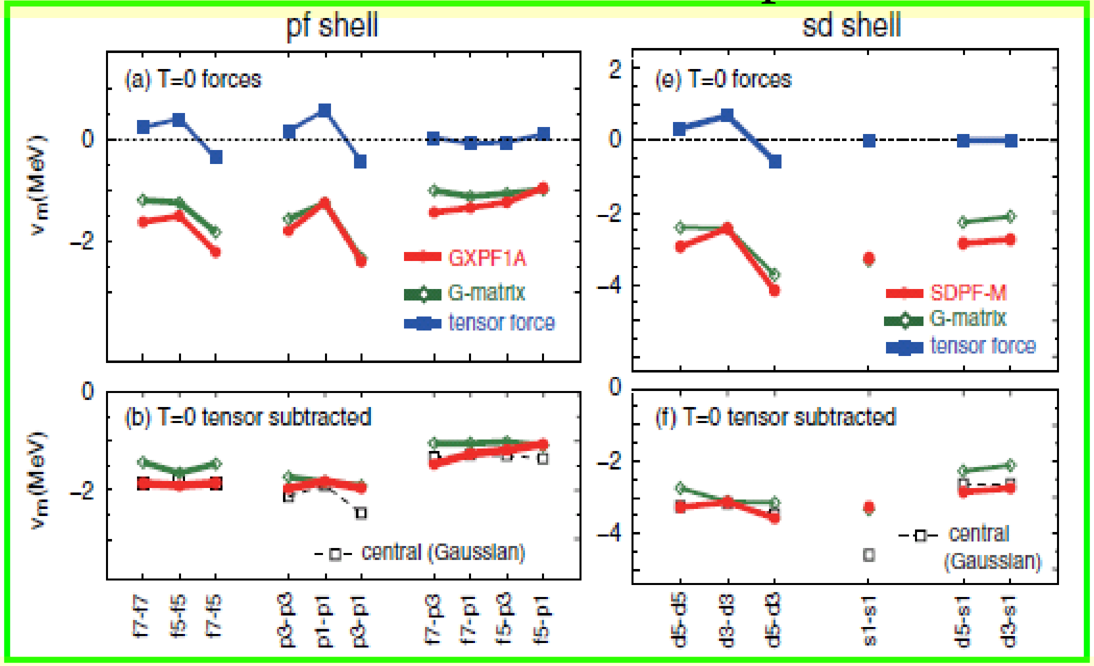

Proper shell evolutions toward drip-lines: Change of magic numbers

p-shell: SFO space; up to 2-3hw,
$g_A^{eff}/g_A=0.95$
B(GT: ^{12}C)_cal = experiment
Vanishing of B(GT: ^{14}C) reproduced

Magnetic moments of p-shell nuclei systematically reproduced

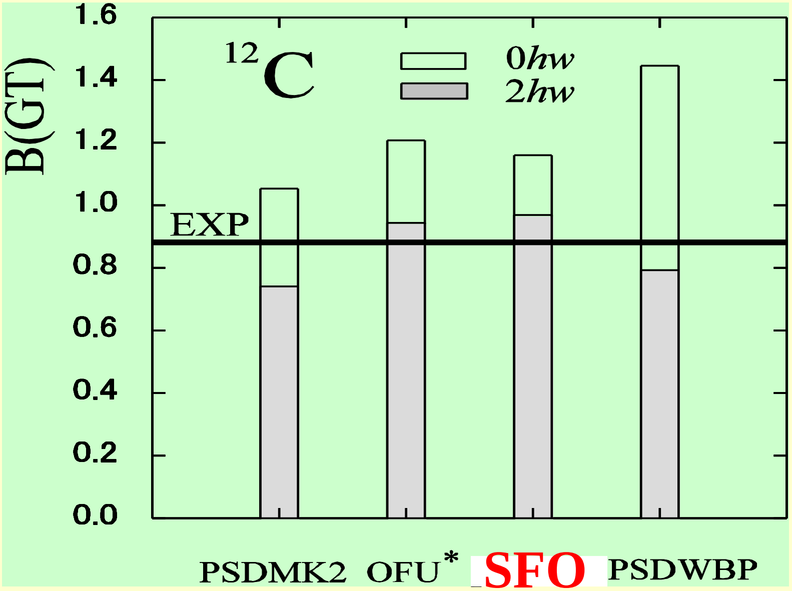

New shell-model Hamiltonians in fp-shell and spin responses

GXPF1: Honma et al., PR C65 (2002); C69 (2004); A = 47-66

KB3: Caurier et al., Rev. Mod. Phys. 77, 427 (2005)

KB3G A = 47-52 KB + monopole corrections

- **Spin properties of fp-shell nuclei are well described**

$B(GT_-)$ for ^{58}Ni $g_A^{eff}/g_A^{free}=0.74$

M1 strength (GXPF1J)

$g_S^{eff}/g_S=0.75\pm0.2$

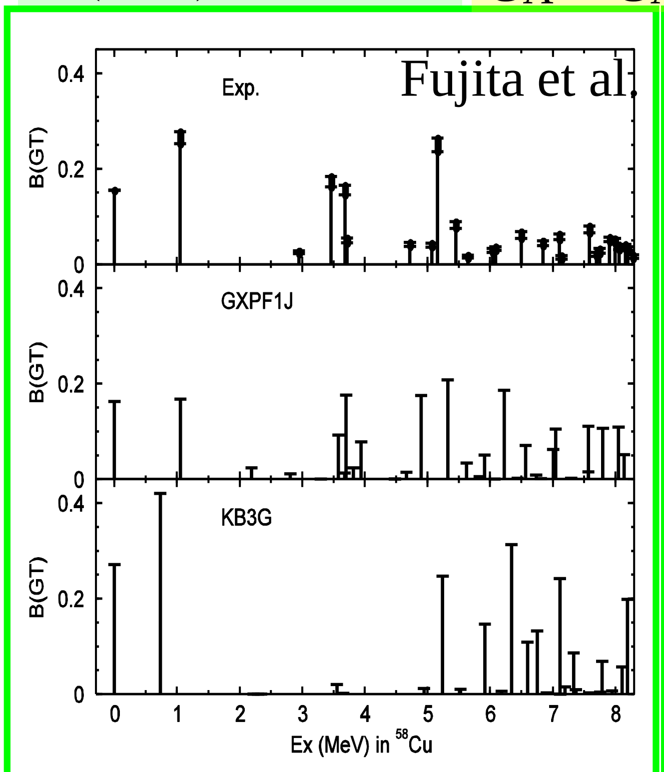

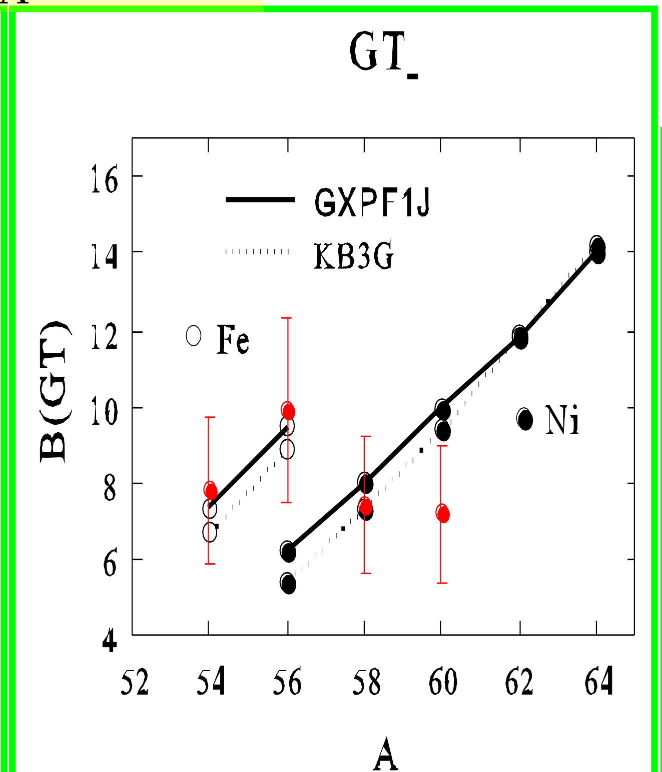

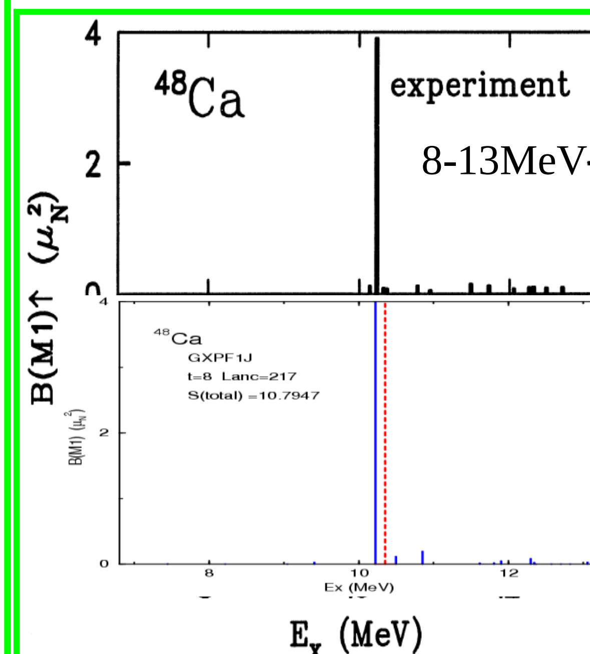

○ ν-nucleus reactions

pf-shell: GXPF1J (Honma et al.)

p-shell: SFO

cf. KB3 Caurier et al.

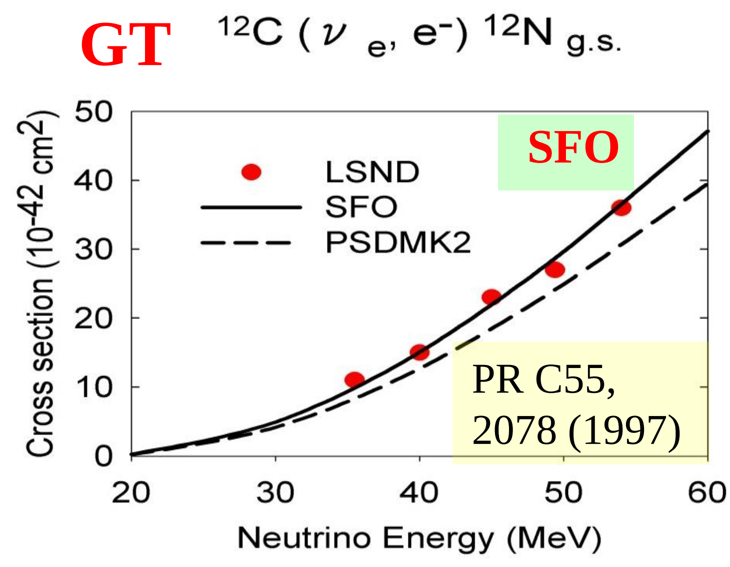

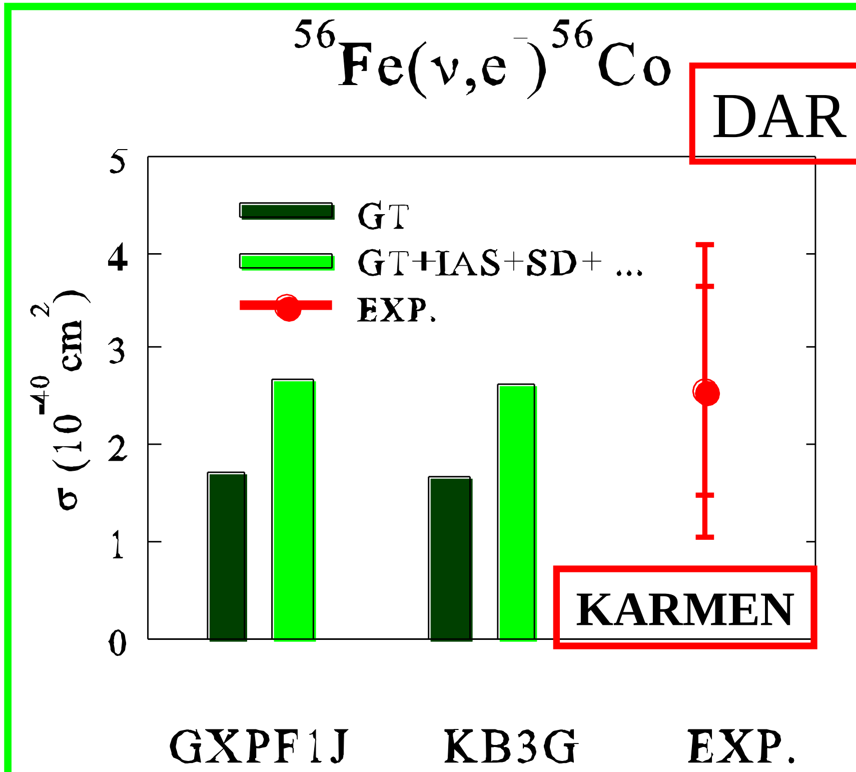

Suzuki, Chiba, Yoshida, Kajino, Otsuka, PR C74, 034307, (2006).

SFO: g_A^{eff}/g_A=0.95

B(GT: 12C)_cal = experiment

(ν, ν'), (ν_e, e^-) SD exc.

SFO reproduces DAR cross sections

$B(GT)=9.5$ $B(GT)_{exp}=9.9\pm2.4$ $B(GT)_{KB3G}=9.0$

SD + … : RPA (SGII)

$$\langle\sigma\rangle_{exp} = (256 \pm 108 \pm 43) \times 10^{-42}\ cm^2.$$

$$\langle\sigma\rangle_{th} = (258 \pm 57) \times 10^{-42}\ cm^2.$$

SM(GXPF1J)+RPA(SGII)	259 x10 $^{-42}$cm^2
RHB+RQRPA(DD-ME2)	263
RPA(Landau-Migdal force)	240

Nucleosynthesis processes of light elements

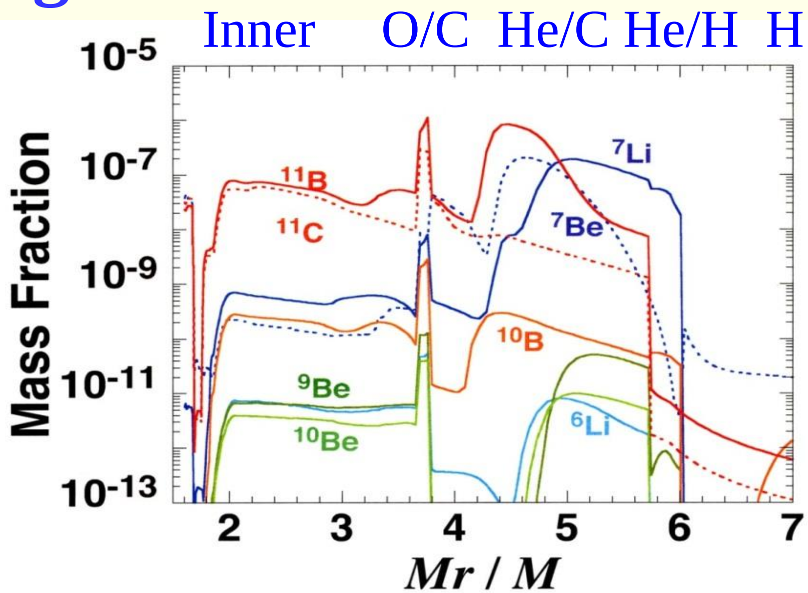

Fig. 4.— Mass fraction distribution of Model 1. The mass fractions of ^{7}Li and ^{7}Be, and ^{11}B and ^{11}C are separated.

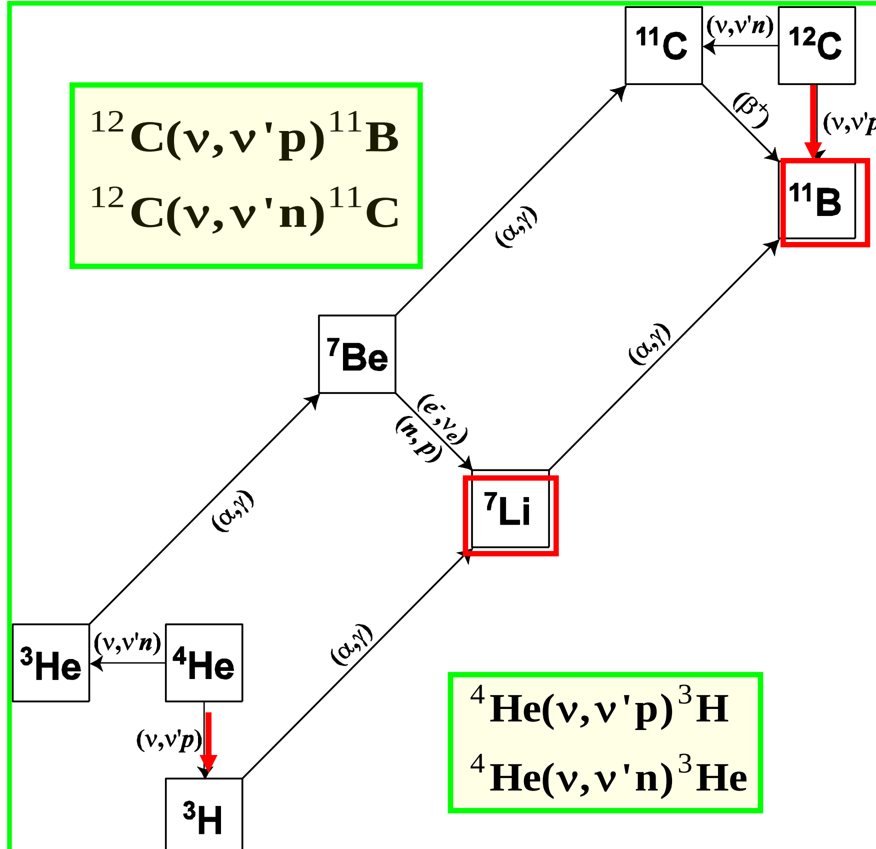

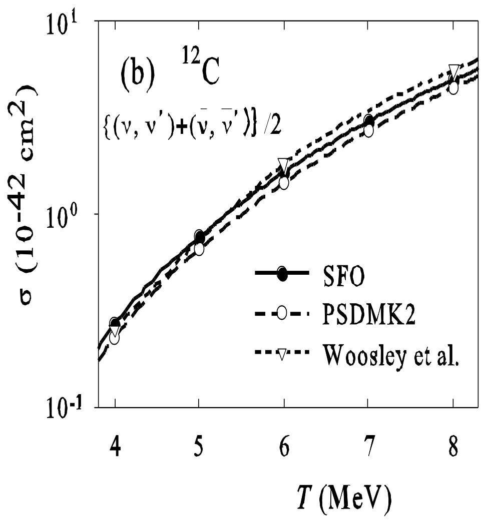

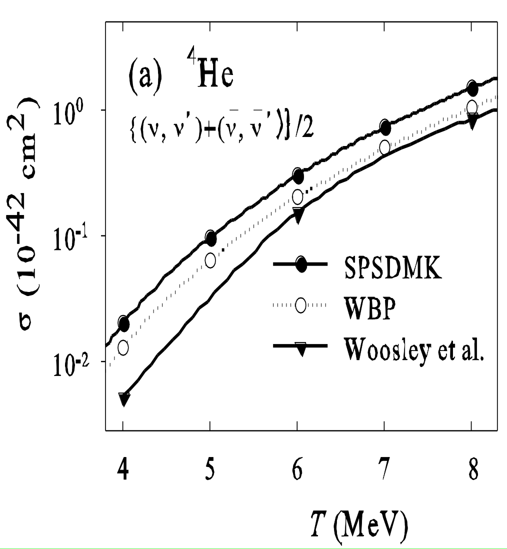

Enhancement of ^{11}B and ^{7}Li abundances in supernova explosions

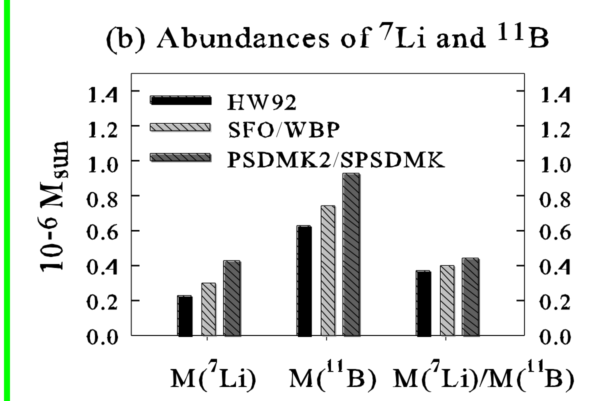

MSW ν oscillations

Normal hierarchy | Inverted hierarchy

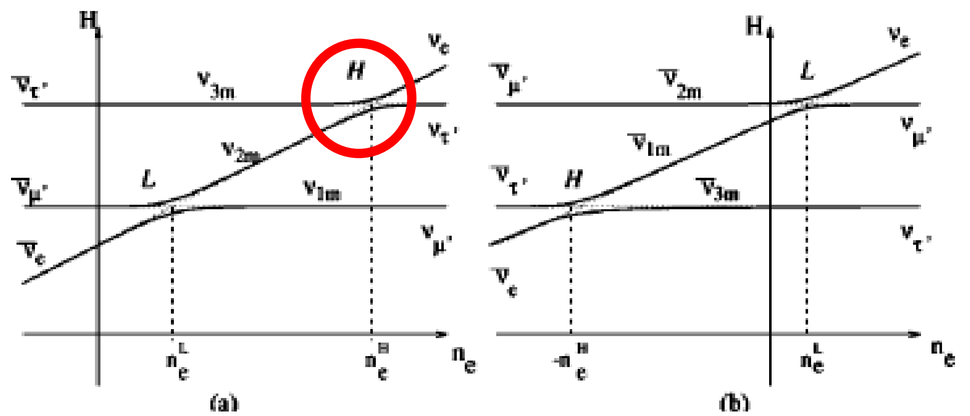

$$\mathrm{Normal-hierarchy}:\nu_\mu,\nu_\tau\rightarrow\nu_e$$

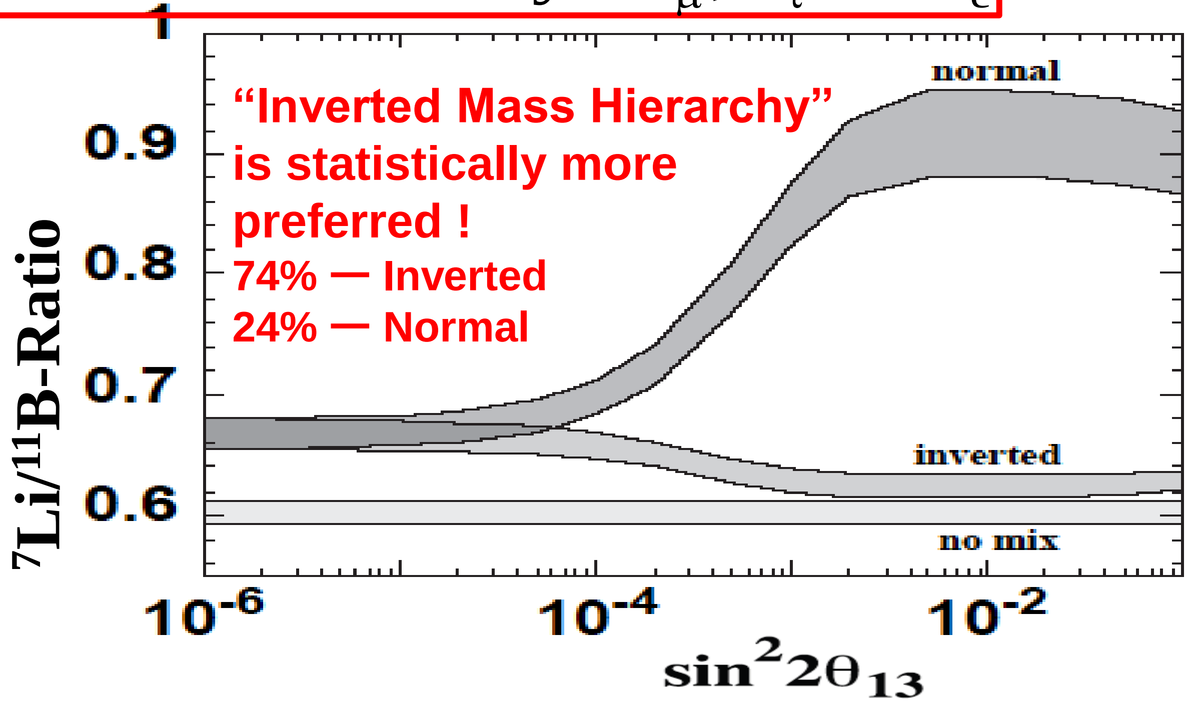

Increase in the rates

^{4}He$(\nu_e,e^-p)^3$He

^{12}C$(\nu_e,e^-p)^{11}$C

in the He layer

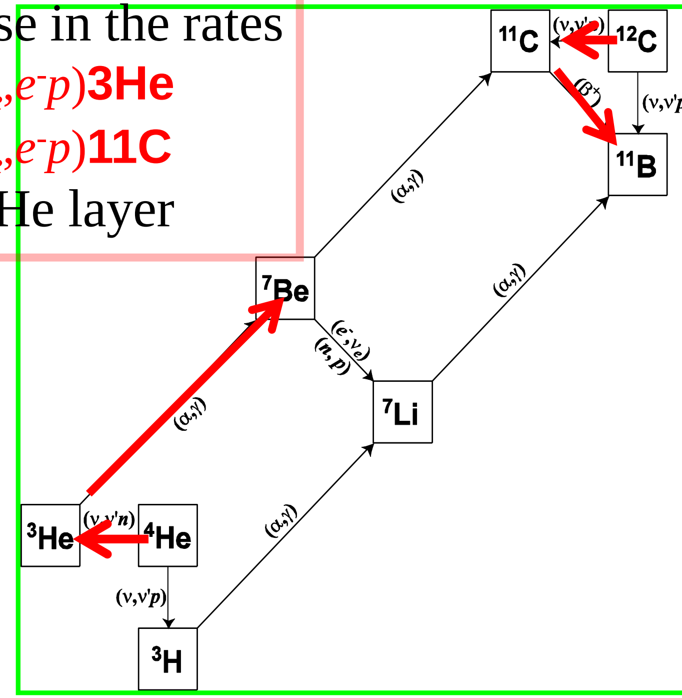

- T2K, MINOS (2011)
- Double CHOOZ, Daya Bay, RENO (2012)

$\sin^2 2\theta_{13} = 0.1$

First Detection of ^{7}Li/^{11}B in SN-grains in Murchison Meteorite

W. Fujiya, P. Hoppe, & U. Ott, ApJ 730, L7 (2011).

Bayesian analysis:

Mathews, Kajino, Aoki and Fujiya, Phys. Rev. D85,105023 (2012).

- Effects of MSW ν-oscillations
  normal hierarchy: high res. + low res. → ^{7}Li/^{11}B enhanced
  inverted-hierarchy: no high-res. → ^{7}Li/^{11}B not enhanced

Supernova X-grains in Murchison meteorite
→ inverted hierarchy is statistically favored

W. Fujiya, P. Hoppe, & U. Ott, ApJ 730, L7 (2011).
Mathews, Kajino, Aoki and Fujiya, Phys. Rev. D85,105023 (2012).

- New ν-^{13}C cross sections with SFO
  ^{13}C is a good target for low-energy ν detection; E<10 MeV

Suzuki, Balantekin and Kajino, PR C86, 015502 (2012)

- New ν-^{16}O cross sections with SFO-tls
  Full inclusion of tensor force in p-sd cross shells:
  tensor → π+ρ LS → σ+ρ+ω

$$\frac{\sigma(^{16}O(\nu,\nu'\alpha p)^{11}B)}{\sigma(^{12}C(\nu,\nu' p)^{11}B)} \approx 20\%$$

^{11}B is produced from ^{16}O also

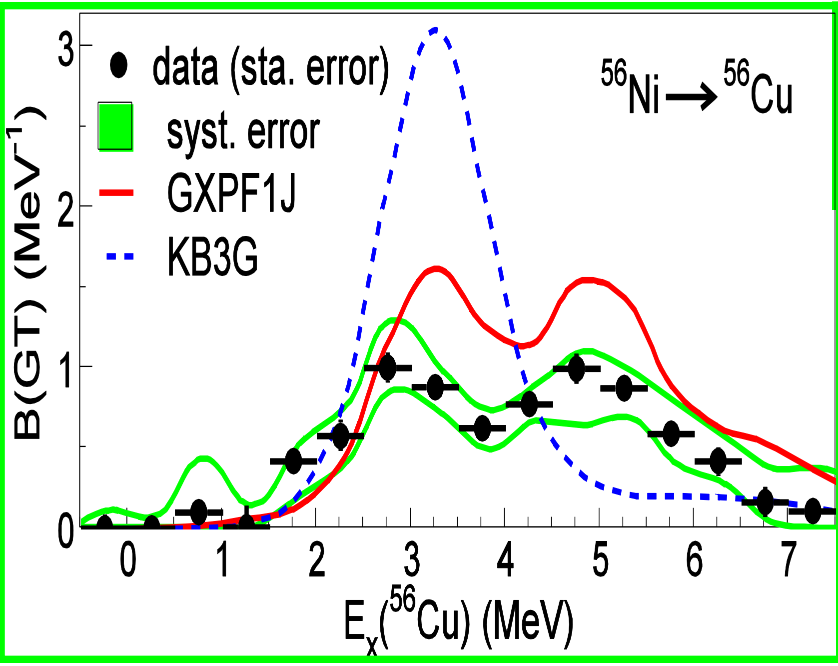

Sasano et al., PRL 107, 202501 (2011)

▪ e-capture rates on ^{56}Ni in stellar environments: $\rho Y_e = 10^7 - 10^{10}\ g/cm^3$

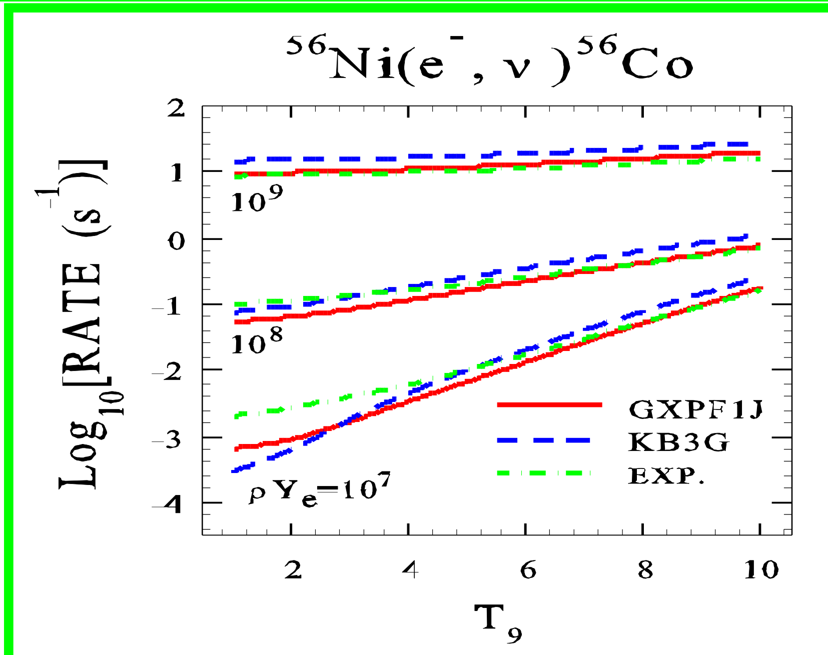

Suzuki, Honma, Mao, Otsuka, Kajino, PR C83, 044619 (2011)

Type-Ia supernova explosion

Accretion of matter to white-dwarf from binary star

→ supernova explosion when white-dwarf mass > Chandrasekhar limit

→ ^{56}Ni (N=Z)

→ ^{56}Ni (e$^-$, ν) ^{56}Co $\quad Y_e = 0.5 \rightarrow \ Y_e < 0.5$ (neutron-rich)

→ production of neutron-rich isotopes; more ^{58}Ni

Decrease of e-capture rate on ^{56}Ni

→ less production of ^{58}Ni.

e-capture rates: GXPF1J < KB3G

←→

Y_e (GXPF1J) > Y_e (KB3G)

Problem of over-production of ^{58}Ni may be solved.

Problem of over-production of ^{58}Ni

THE ASTROPHYSICAL JOURNAL SUPPLEMENT SERIES, 125:439–462, December

NUCLEOSYNTHESIS IN CHANDRASEKHAR MASS MODELS FOR TYPE Ia SUPERNOVAE AND CONSTRAINTS ON PROGENITOR SYSTEMS AND BURNING-FRONT PROPAGATION

KOICHI IWAMOTO,[1,2,3] FRANZISKA BRACHWITZ,[4] KEN'ICHI NOMOTO,[1,2,3] NOBUHIRO KISHIMOTO,[1]
HIDEYUKI UMEDA,[2,3] W. RAPHAEL HIX,[3,5] AND FRIEDRICH-KARL THIELEMANN[3,4,5]

Received 1999 January 11; accepted 1999 July 29

and ignition densities to put new constraints on the above key quantities. The abundance of the Fe group, in particular of neutron-rich species like ^{48}Ca, ^{50}Ti, ^{54}Cr, ^{54,58}Fe, and ^{58}Ni, is highly sensitive to the electron captures taking place in the central layers. The yields obtained from such a slow central

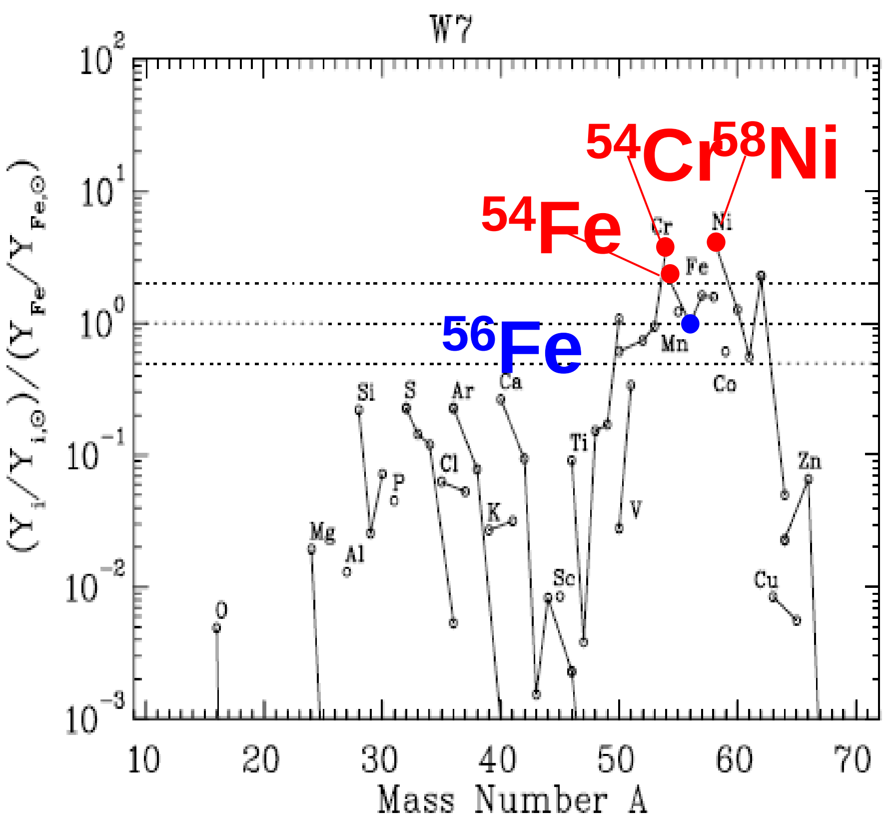

Famiano

NSE(Nuclear Statistical Equilibrium) calculation

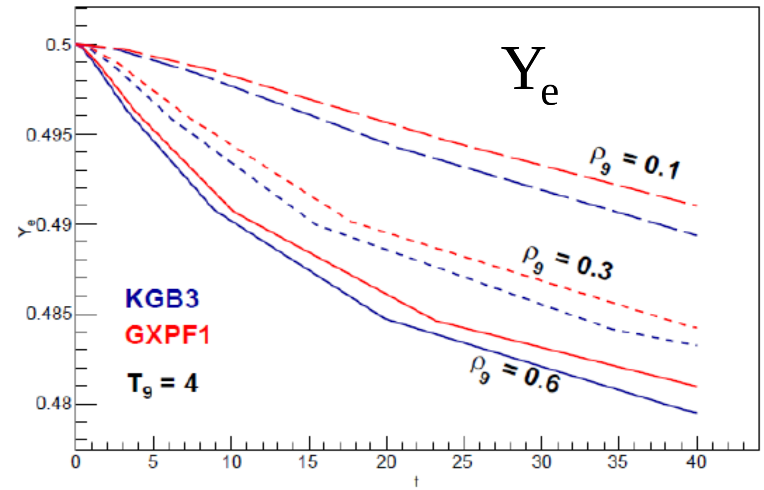

Ratio between ^{58}Ni / ^{56}Ni

GXPF1 -> ^{58}Ni/^{56}Ni decreases

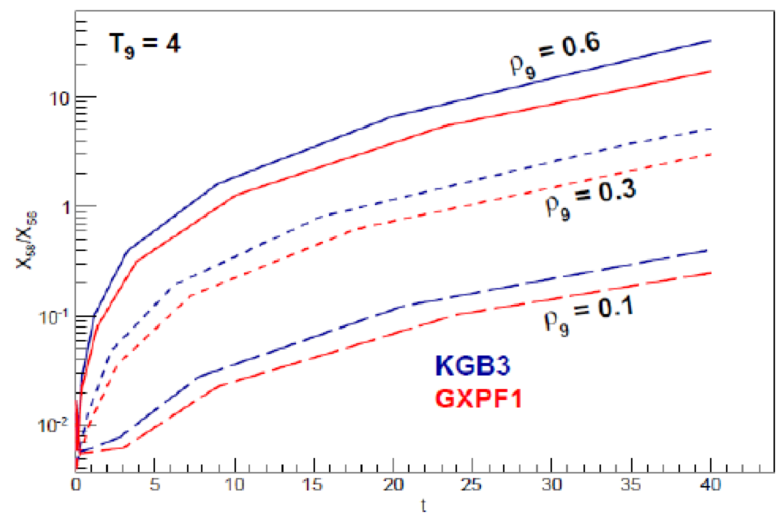

○Evolution of 8-10$M_\odot$ stars and nuclear URCA processes

- M=0.5 ～8$M_\odot$
  He burning → C-O core → C-O white dwarfs
- M >10$M_\odot$
  → Fe core → core-collapse supernova explosion
- M=8$M_\odot$ ～ 10$M_\odot$
  C burning → O-Ne-Mg core
  → (1) O-Ne-Mg white dwarf (WD)
  → (2) e-capture supernova explosion (collapse of O-Ne-Mg core induced by e-capture) with neutron star (NS) remnant
  → (3) core-collapse (iron-core collapse) supernova explosion with NS (neon burning shell propagates to the center)

Fate of the star is sensitive to its mass and nuclear e-capture and β–decay rates; Cooling of O-Ne-Mg core by nuclear URCA processes determines (2) or (3).

Nomoto and Hashimoto, Phys. Rep. 163, 13 (1988)
Miyaji, Nomoto, Yokoi, and Sugimoto, Pub. Astron. Soc. Jpn. 32, 303 (1980)
Nomoto, Astrophys. J. 277, 791 (1984); ibid. 322, 206 (1987)

▪Detailed e-capture and beta-decay rates for URCA nuclear pairs in 8-10 solar-mass stars

Nuclear URCA process

$$^{23}Na + e^- \rightarrow {}^{23}Ne + \nu$$

$$^{23}Ne \rightarrow {}^{23}Na + e^- + \overline{\nu}$$

$$^{25}Mg + e^- \rightarrow {}^{25}Na + \nu$$

$$^{25}Na \rightarrow {}^{25}Mg + e^- + \overline{\nu}$$

$$^{27}Al + e^- \rightarrow {}^{27}Mg + \nu$$

$$^{27}Mg \rightarrow {}^{27}Al + e^- + \overline{\nu}$$

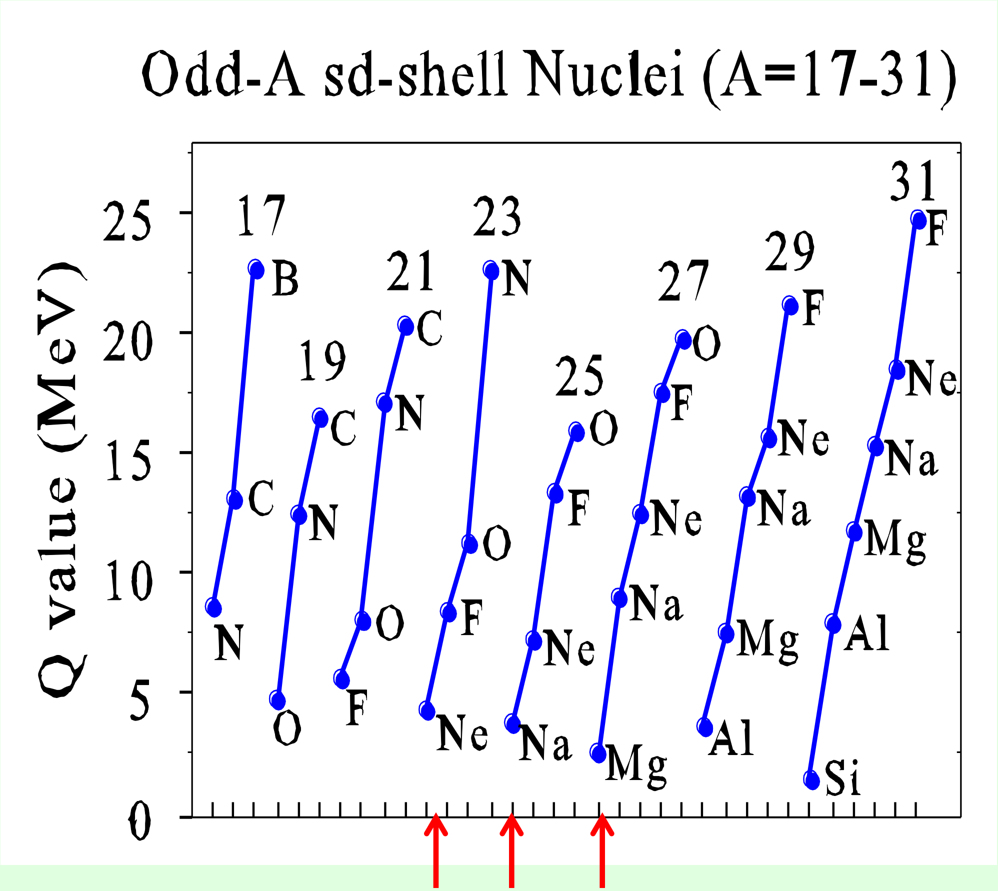

Cooling of O-Ne-Mg core of stars

→ 'e-cap.SNe' or 'core-collapse SNe'

sd-shell: USDB Brown and Richter, PR C74, 034315 (2006)

Richter, Mkhize, Brown, PR C78, 064302 (2008)

- e-capture rates at high densities and high temperatures

$$\lambda = \frac{\ln 2}{6146(s)} \sum_i W_i \sum_f B(\mathrm{GT}; i \to f) \times \int_{\omega_{\min}}^{\infty} \omega p (Q_{ij} + \omega)^2 F(Z, \omega) S_e(\omega) d\omega,$$

$$Q_{if} = (M_p c^2 - M_d c^2 + E_i - E_f)/m_e c^2,$$

$$W_i = (2J_i + 1) e^{-E_i/kT} / \sum_i (2J_i + 1) e^{-E_i/kT},$$

$$B_{ij}(GT) = \left(\frac{g_A}{g_V}\right)^2_{\text{eff}} \frac{\langle j || \sum_k \sigma^k t^k_{\pm} || i \rangle^2}{2J_i + 1},$$

$$B_{ij} = B_{ij}(F) + B_{ij}(GT).$$

$$B_{ij}(F) = \frac{\langle j || \sum_k t^k_{\pm} || i \rangle^2}{2J_i + 1}.$$

$$S_e = \frac{1}{\exp\left(\frac{E_e - \mu_e}{kT}\right) + 1},$$

$$\mu_p = -\mu_e.$$

$$\rho Y_e = \frac{1}{\pi^2 N_A} \left(\frac{m_e c}{\hbar}\right)^3 \int_0^{\infty} (S_e - S_p) p^2 dp,$$

Y_e = No. electrons/No. baryons

TABLE III. Electron chemical potential μ_e (in units of MeV) at high densities, $\rho Y_e = 10^7$–10^{10} g/cm^3, and high temperatures, $T = T_9 \times 10^9$ K.

ρY_e (g/cm^3)	T_9									
	1	2	3	4	5	6	7	8	9	10
10^7	1.200	1.133	1.021	0.870	0.698	0.534	0.404	0.310	0.244	0.196
10^8	2.437	2.406	2.355	2.283	2.192	2.081	1.952	1.808	1.653	1.493
10^9	5.176	5.162	5.138	5.105	5.062	5.010	4.948	4.877	4.797	4.708
10^{10}	11.116	11.109	11.098	11.083	11.063	11.039	11.011	10.978	10.940	10.898

- β-decay

$$\Phi_{ij}^{\beta^-} = \int_1^{Q_{ij}} wp(Q_{ij} - w)^2 F(Z+1, w)(1 - S_e(w)) \, d\omega$$

$$^{23}Na + e^- \rightarrow {}^{23}Ne + \nu$$

$$^{23}Ne \rightarrow {}^{23}Na + e^- + \overline{\nu}$$

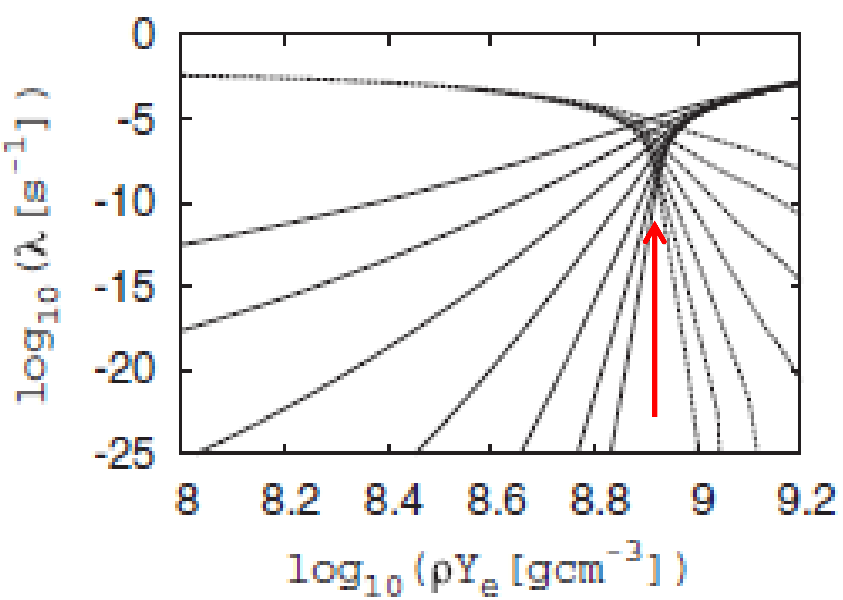

e-capture rates increase as density increases, while β-decay rates decrease as density increases.

There is a density where both the rates are balanced and depends little on T.
→ URCA density

URCA density at $\log_{10} \rho Y_e = 8.92$ for $A = 23$

$\log_{10} T = 8$ to 9.2 in steps of 0.2

$(^{25}Na, ^{25}Mg)$

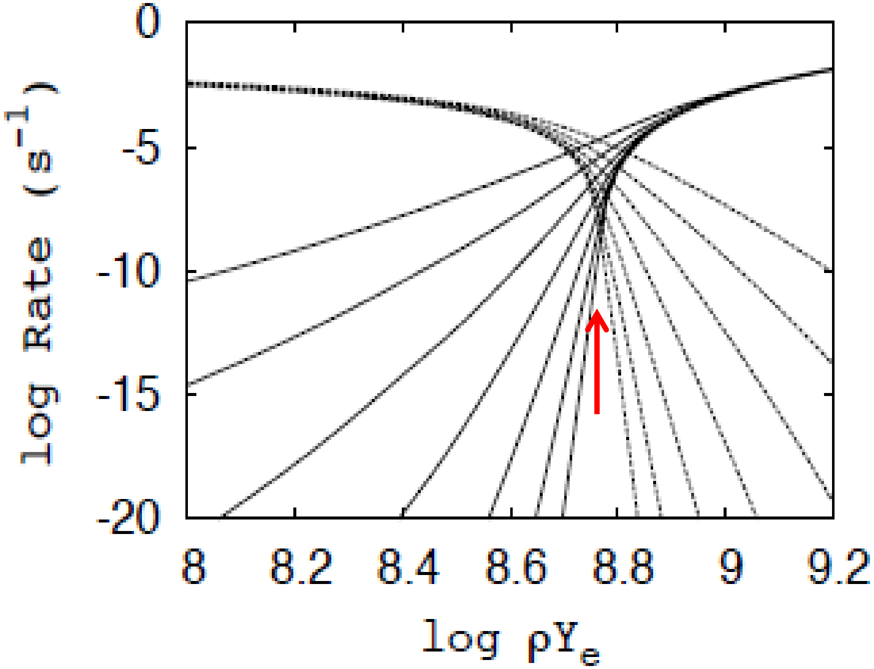

$(^{27}Mg, ^{27}Al)$

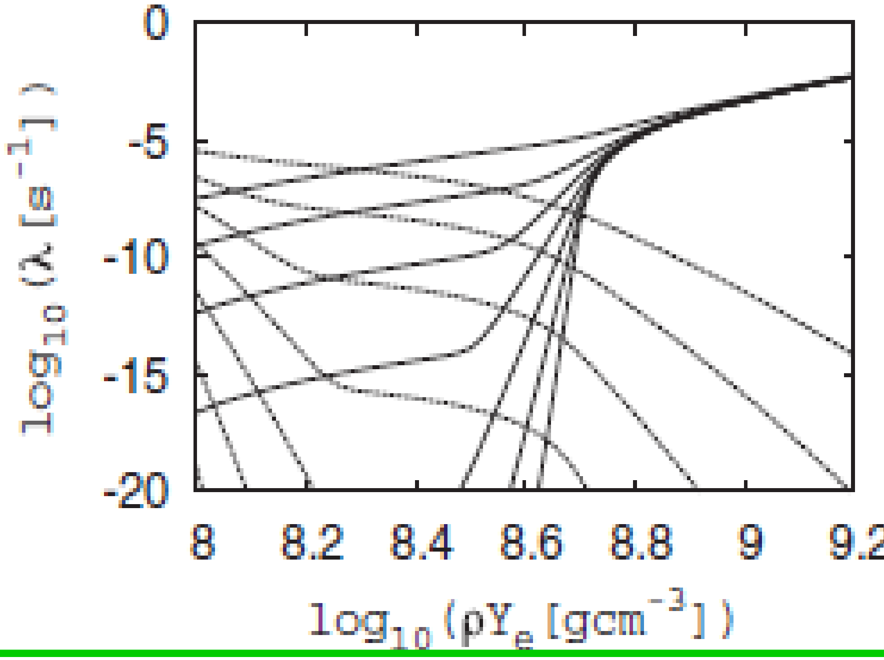

The temperature steps are shown in the range of $\log_{10} T$ = 8 to 9.2 in steps of 0.2.

URCA density at $\log_{10} \rho Y_e = 8.78$

No clear URCA density for A=27

The ground-state spin of ^{27}Mg is 1/2+ and the ground-state spin of ^{27}Al is 5/2+ and the GT matrix element is zero.

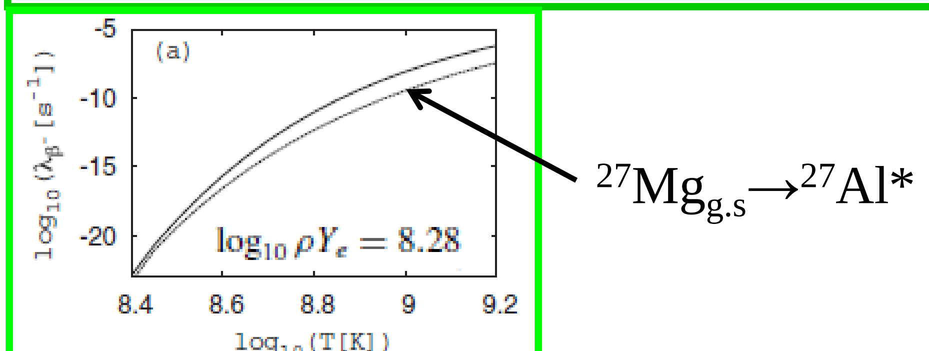

Cooling of O-Ne-Mg core by the nuclear URCA processes

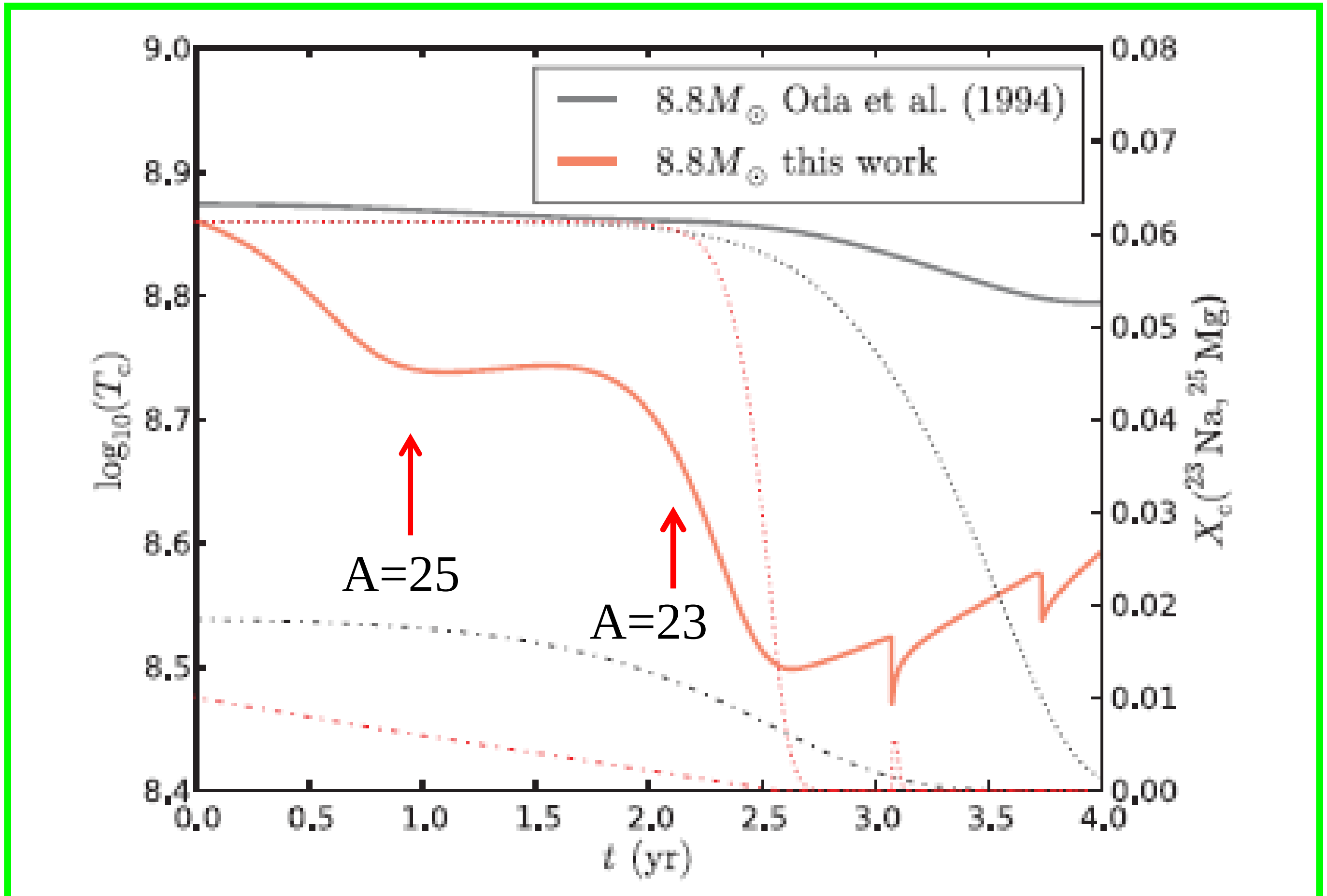

8.8$M_\odot$ star collapses triggered by subsequent e-capture on ^{24}Mg and ^{20}Ne (e-capture supernova explosion)

Toki, Suzuki, Nomoto, Jones and Hirschi, PR C 88, 015806 (2013)

Table 1
Summary of Model Properties

	8.2 $M_\odot$	8.7 $M_\odot$	8.75 $M_\odot$	8.8 $M_\odot$	9.5 $M_\odot$	12.0 $M_\odot$
$M^{C}_{ign}/M_\odot$ [a]	0.15	0.00	0.00	0.00	0.00	0.00
$M^{Ne}_{ign}/M_\odot$ [b]	…	…	…	0.93	0.42	0.00
T^{Ne}_{ign}/GK [c]	…	…	…	1.318	1.311	1.324
ψ^{Ne}_{c} [d]	…	…	…	46.0	15.2	5.6
$\rho^{Ne}_{c}/\mathrm{g\ cm^{-3}}$ [e]	…	…	…	3.343×10^8	7.396×10^7	1.730×10^7
$M_{tot}/M_\odot$ [f]	7.299	7.910	8.572	8.544	9.189	11.338
$M_{env}/M_\odot$ [g]	6.031	6.559	7.210	7.174	6.702	8.023
$M_{He}/M_\odot$ [h]	1.26721	1.35092	1.36230	1.36967	2.48733	3.31580
$M_{CO}/M_\odot$ [i]	1.26695	1.35086	1.36227	1.36964	1.49246	1.88602
Remnant	ONe WD	ONe WD/NS	NS	NS	NS	NS
SN type	…	…/EC-SN (IIP)	EC-SN (IIP)	EC-SN (IIP)	CC-SN (IIP)	CC-SN (IIP)

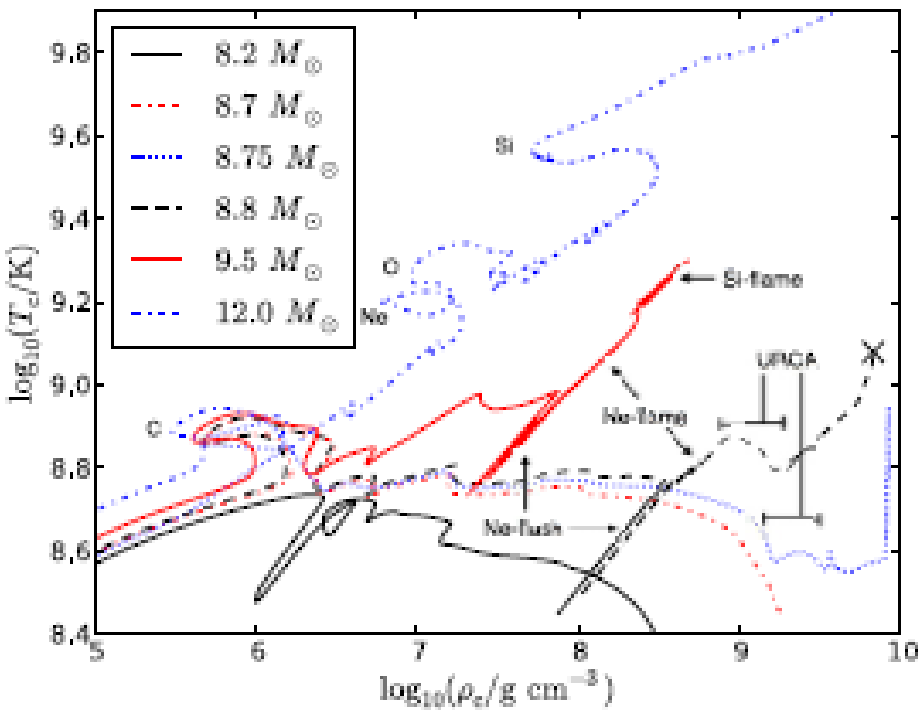

Jones et al., Astrophys. J. 772, 150 (2013)

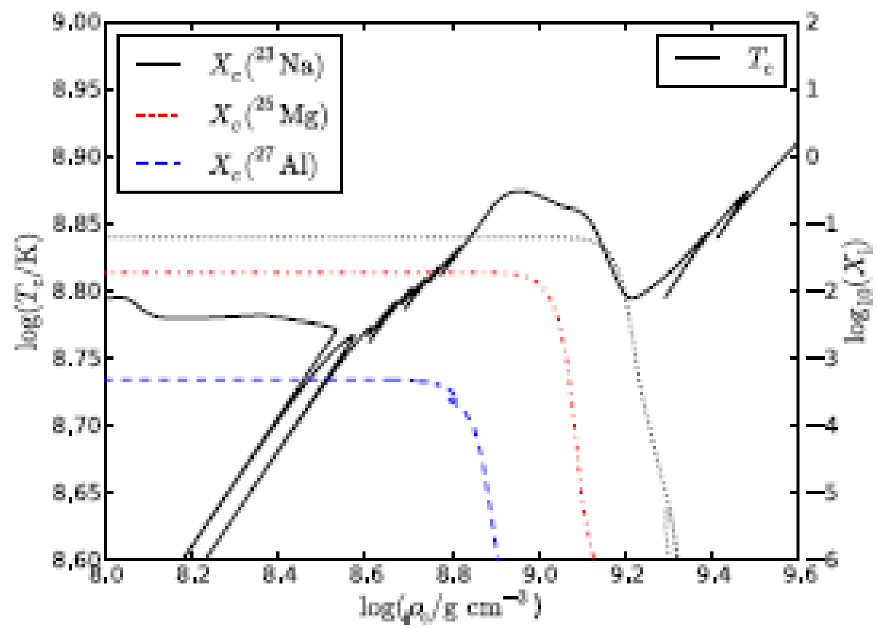

LETTER Nature 505, 65 (2014)

doi:10.1038/nature12757

Strong neutrino cooling by cycles of electron capture and β^- decay in neutron star crusts

H. Schatz[1,2,3], S. Gupta[4], P. Möller[2,5], M. Beard[2,6], E. F. Brown[1,2,3], A. T. Deibel[2,3], L. R. Gasques[7], W. R. Hix[8,9], L. Keek[1,2,3], R. Lau[1,2,3], A. W. Steiner[2,10] & M. Wiescher[2,6]

Table 1 | Electron-capture/β^--decay pairs with highest cooling rates

Electron-capture/β^--decay pair		Density†	Chemical potential†	Luminosity‡
Parent	Daughter*	(10^{10} g cm^{-3})	(MeV)	(10^{36} erg s^{-1})
^{29}Mg	^{29}Na	4.79	13.3	24
^{55}Ti	^{55}Sc, ^{55}Ca	3.73	12.1	11
^{31}Al	^{31}Mg	3.39	11.8	8.8
^{33}Al	^{33}Mg	5.19	13.4	8.3
56Ti	56Sc	5.57	13.8	3.5
^{57}Cr	^{57}V	1.22	8.3	1.6
^{57}V	^{57}Ti, ^{57}Sc	2.56	10.7	1.6
^{63}Cr	^{63}V	6.82	14.7	0.97
^{105}Zr	^{105}Y	3.12	11.2	0.92
^{59}Mn	^{59}Cr	0.945	7.6	0.88
^{103}Sr	^{103}Rb	5.30	13.3	0.65
^{96}Kr	^{96}Br	6.40	14.3	0.65
^{65}Fe	^{65}Mn	2.34	10.3	0.60
^{65}Mn	^{65}Cr	3.55	11.7	0.46

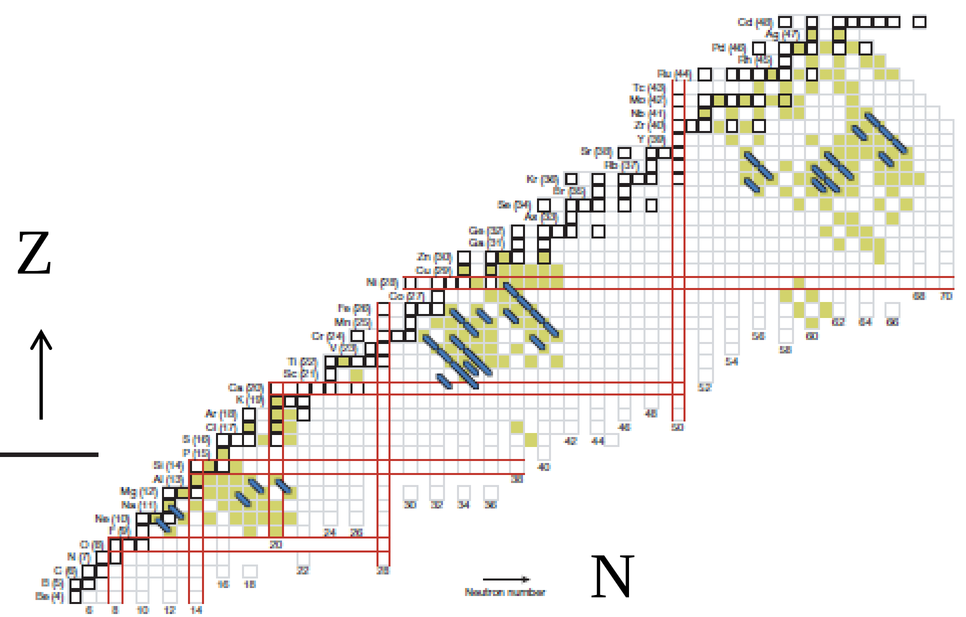

Figure 2 | Electron-capture/β^--decay pairs on a chart of the nuclides. The thick blue lines denote electron-capture/β^--decay pairs that would generate a strong neutrino luminosity in excess of 5×10^{34} erg s^{-1} at $T = 0.51$ GK for a composition consisting entirely of the respective electron-capture/β^--decay pair. They largely coincide with regions where allowed electron-capture and β^--decay transitions are predicted to populate low-lying states and subsequent electron capture is blocked (shaded squares, see also the discussion in ref. 3). These are mostly regions between the closed neutron and proton shells (pairs of horizontal and vertical red lines), where nuclei are significantly deformed (see Supplementary Information section 4). Nuclides that are β^--stable under terrestrial conditions are shown as squares bordered by thicker lines. Nuclear charge numbers are indicated in parentheses next to element symbols.

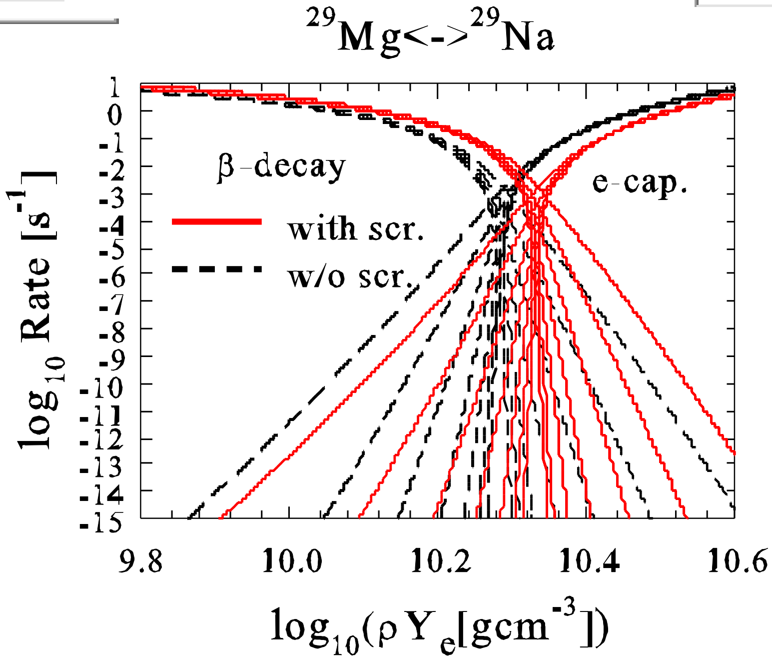

29Mg<->29Na
β-decay
e-cap.
with scr.
w/o scr.
log10 Rate [s-1]
log10(ρYe[gcm-3])

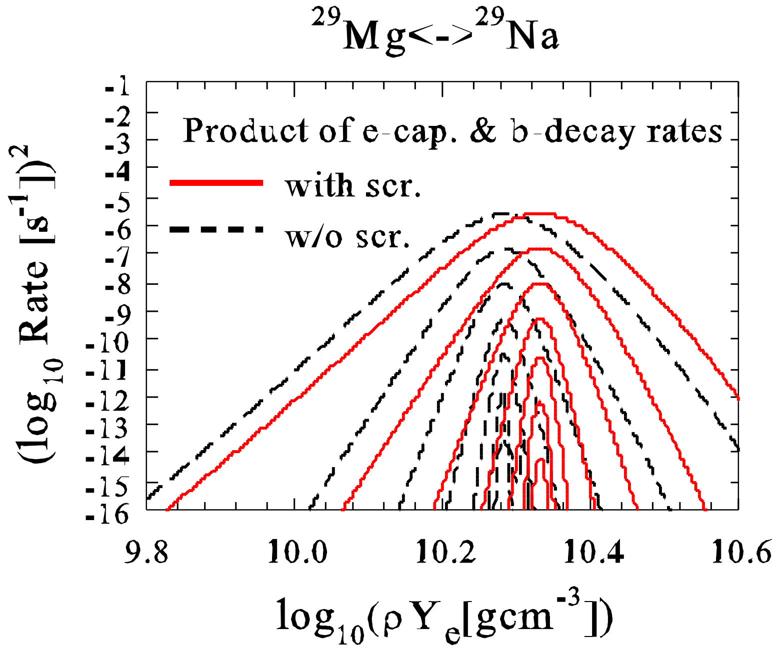

29Mg<->29Na
Product of e-cap. & b-decay rates
with scr.
w/o scr.
(log10 Rate [s-1])2
log10(ρYe[gcm-3])

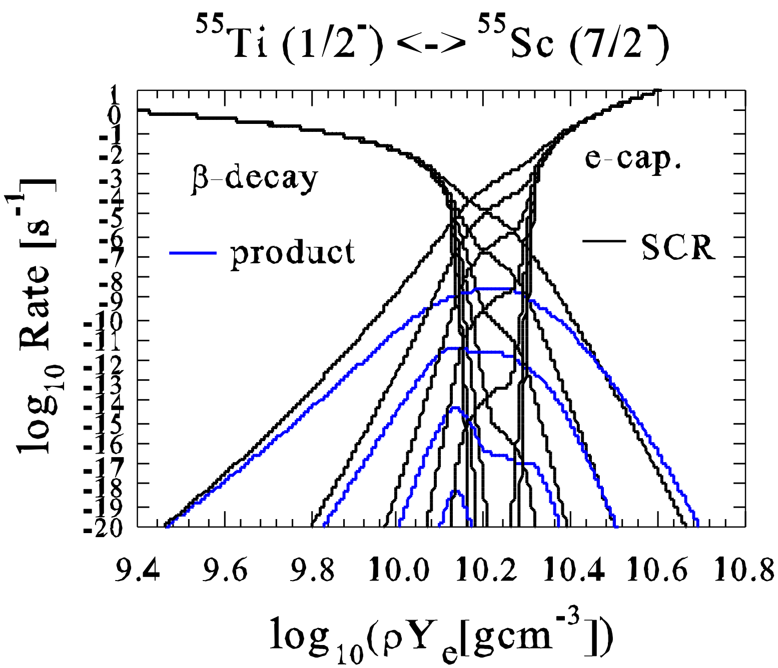

55Ti (1/2-) <-> 55Sc (7/2-)
β-decay
e-cap.
product
SCR
log10 Rate [s-1]
log10(ρYe[gcm-3])

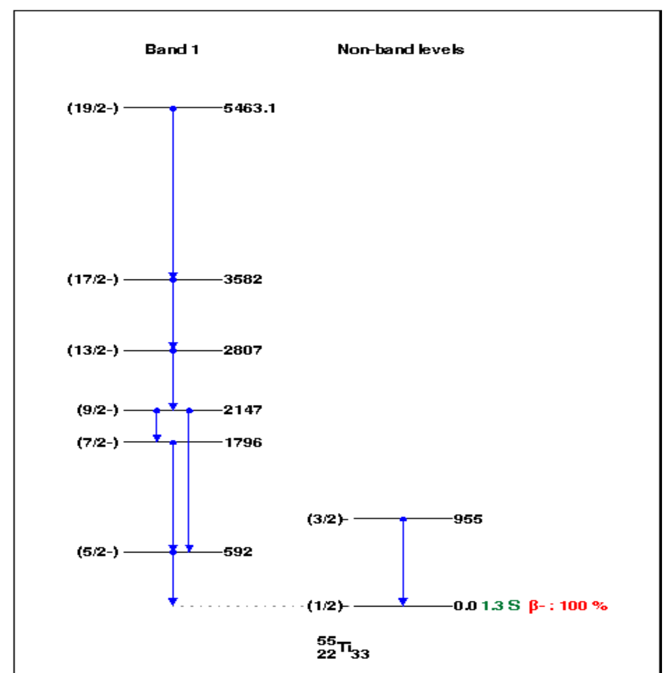

Band 1
Non-band levels
(19/2-) 5463.1
(17/2-) 3582
(13/2-) 2807
(9/2-) 2147
(7/2-) 1796
(3/2)- 955
(5/2-) 592
(1/2)- 0.0 1.3 S β-: 100 %
55 22 Ti 33

○ Beta-Decays of r-process waiting-point nuclei at N=126

R-process

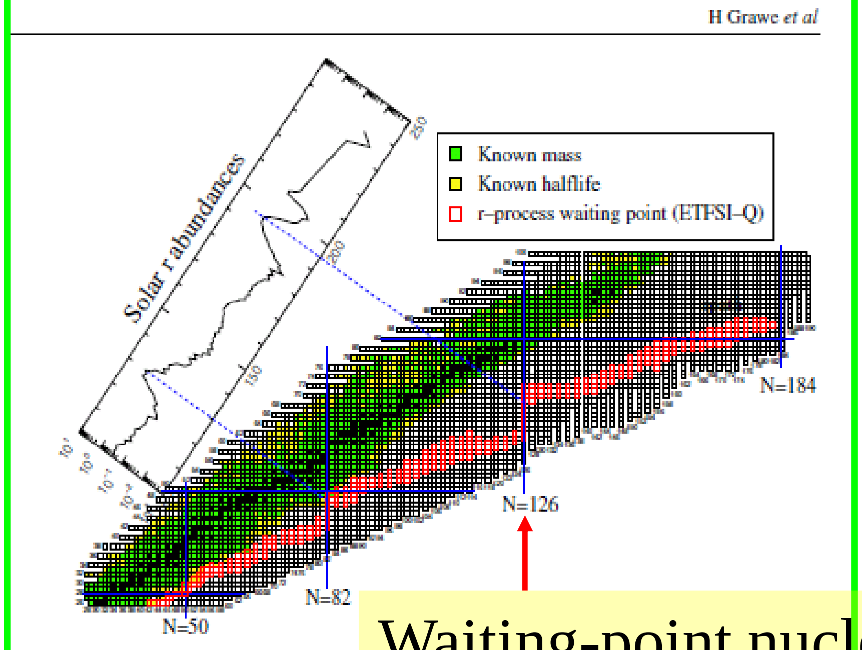

Waiting-point nuclei

Figure 18. The figure shows the range of r-process paths, defined by their waiting point nuclei. After decay to stability the abundance of the r-process progenitors produce the observed solar r-process abundance distribution. The r-process paths run generally through neutron-rich nuclei with experimentally unknown masses and half lives. In this calculation a mass formula based on the ETFSI model and special treatment of shell quenching [79] has been adopted (courtesy of Kratz and Schatz).

Half-lives of N=126 isotones
GT + FF (first-forbidden)

Shell-model

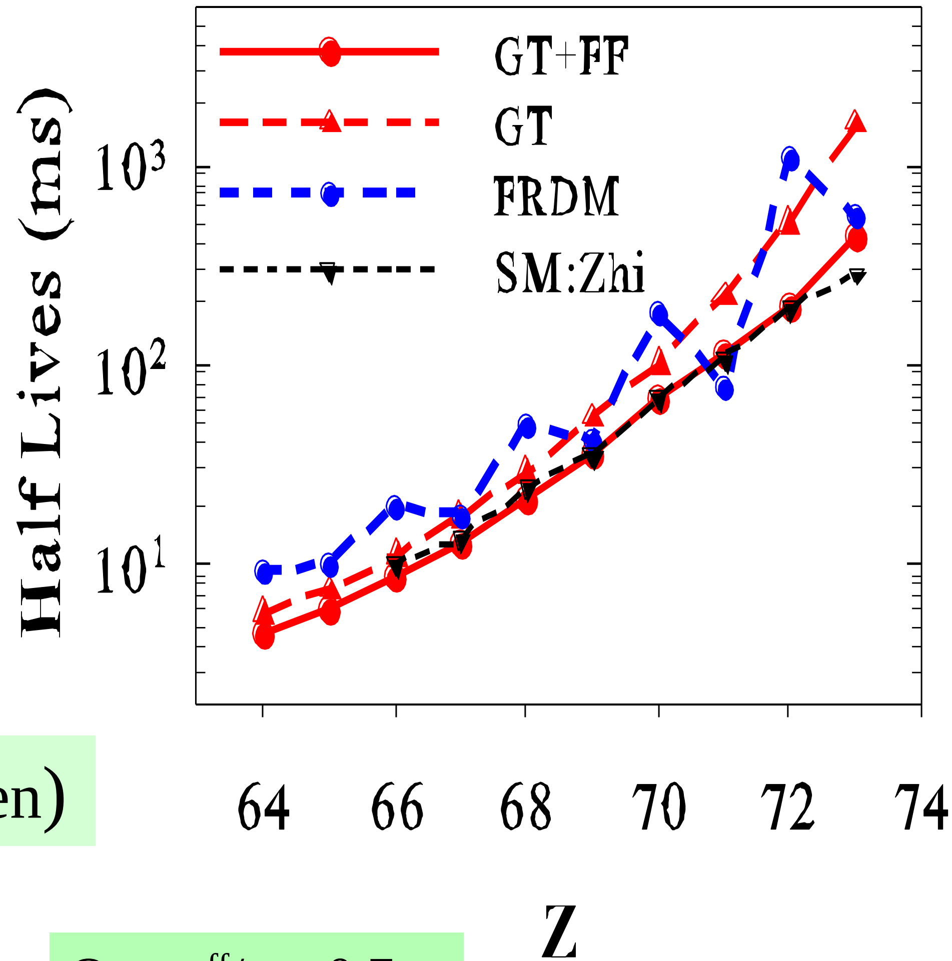

Beta-decay: GT + FF (first-forbidden)

Suzuki, Yoshida, Kajino, Otsuka,
PR C85, 014802 (2012)

$Q=g_A^{eff}/g_A=0.7$

r-process nucleosynthesis up to Th and U

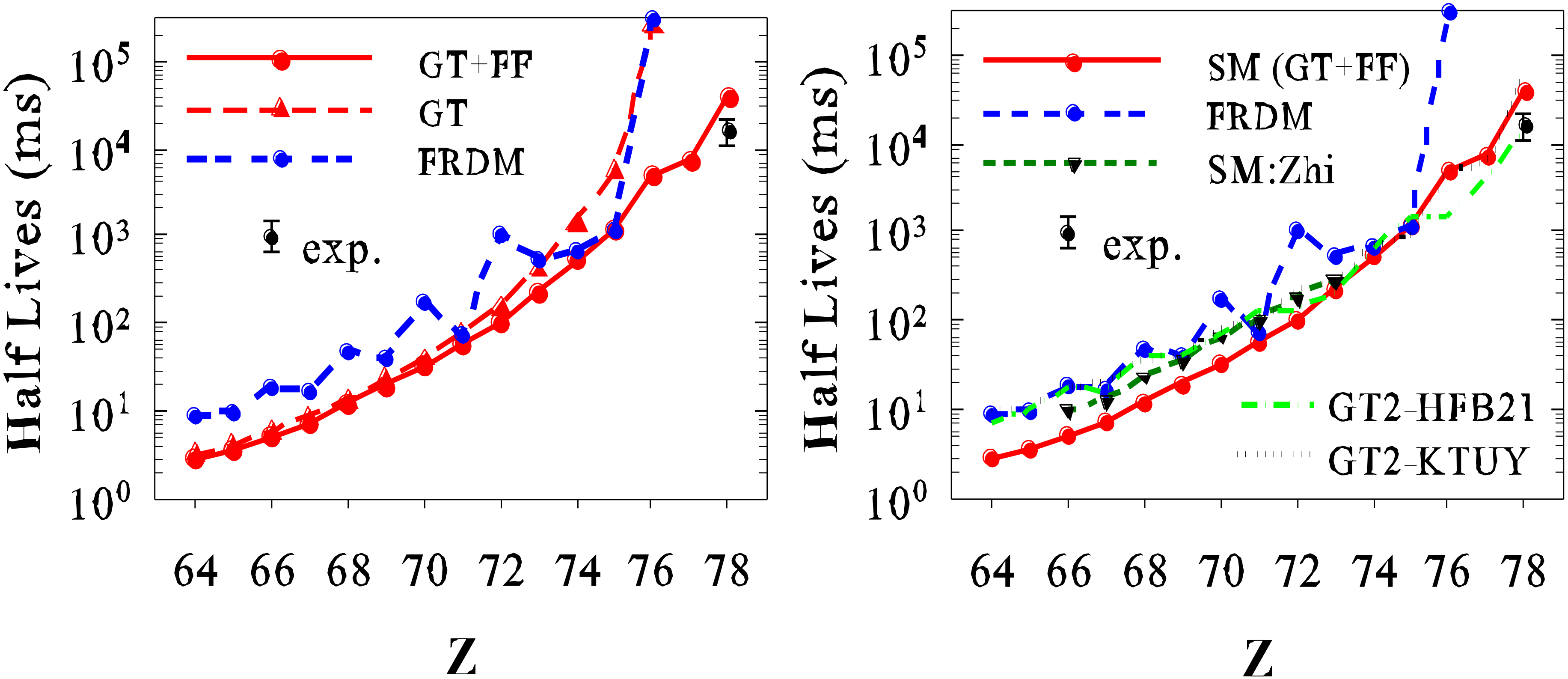

GT: $q(g_A)=0.7$

FF: $q(g_A)=0.34$, $q(g_V)=0.67$

Z=78: ^{204}Pt $t_{1/2}$(exp) =16 +6/-5 s Morales et al., PRL 113 (2014)

ν-driven-wind model in core-collapse SNe

Yoshida

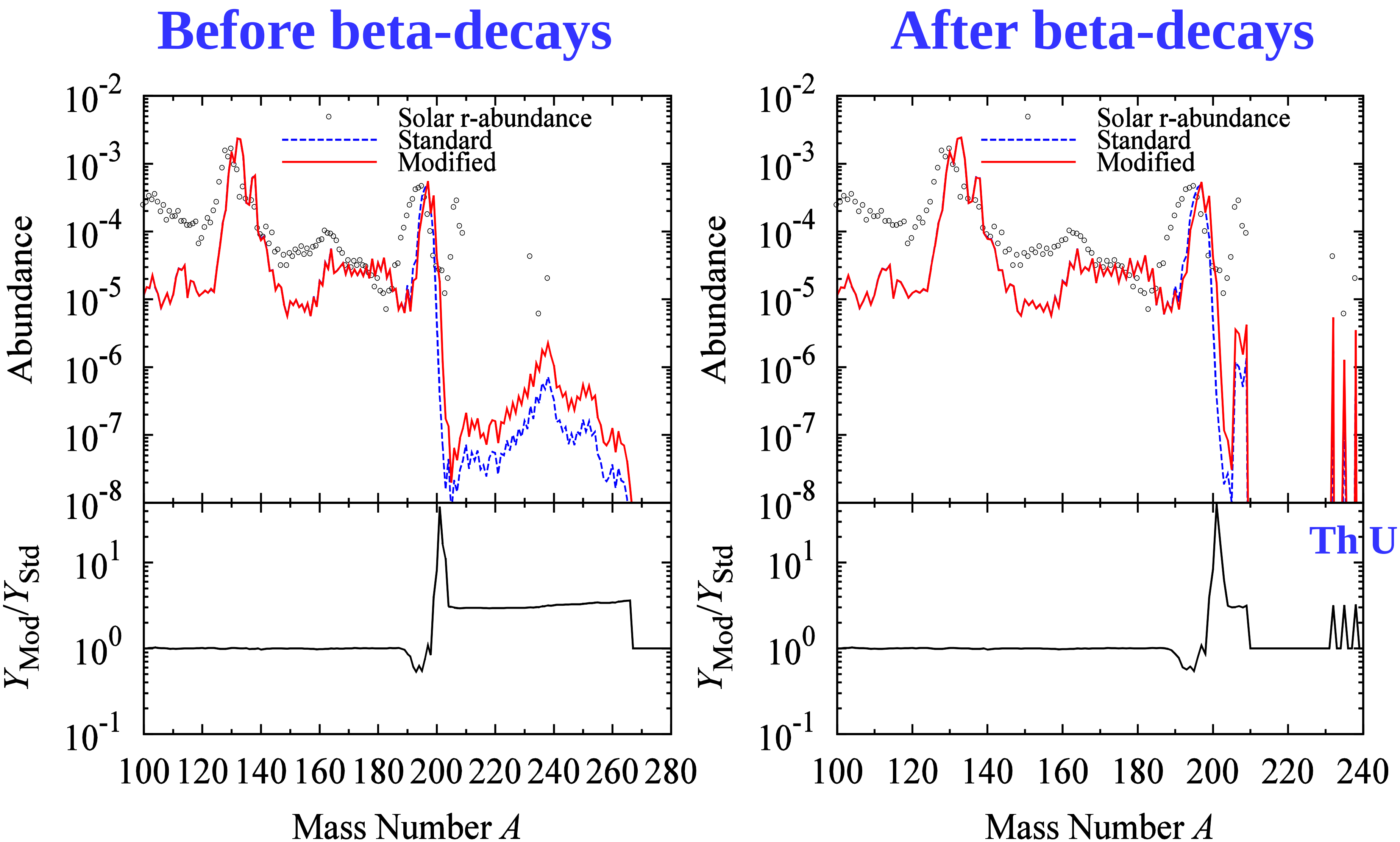

Cold case: $T_f = 1 \times 10^8$ K

Before beta-decays

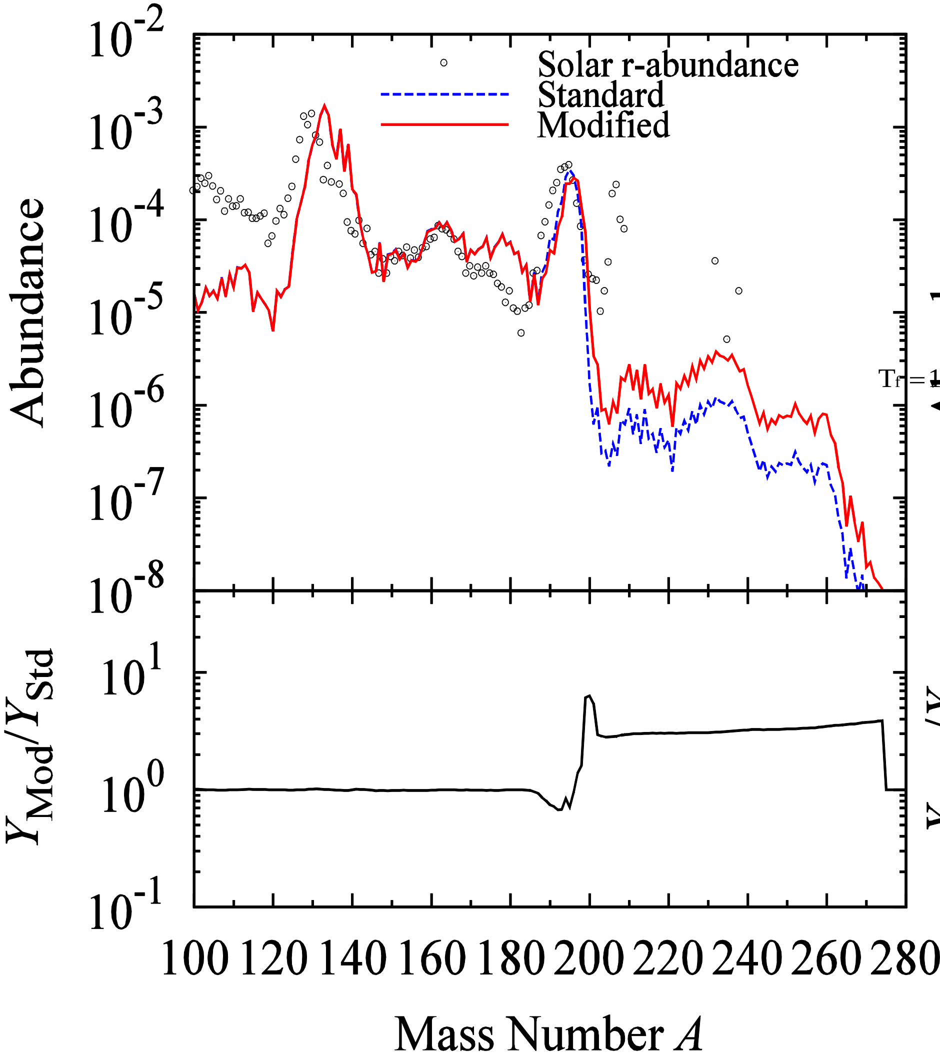

After beta-decays

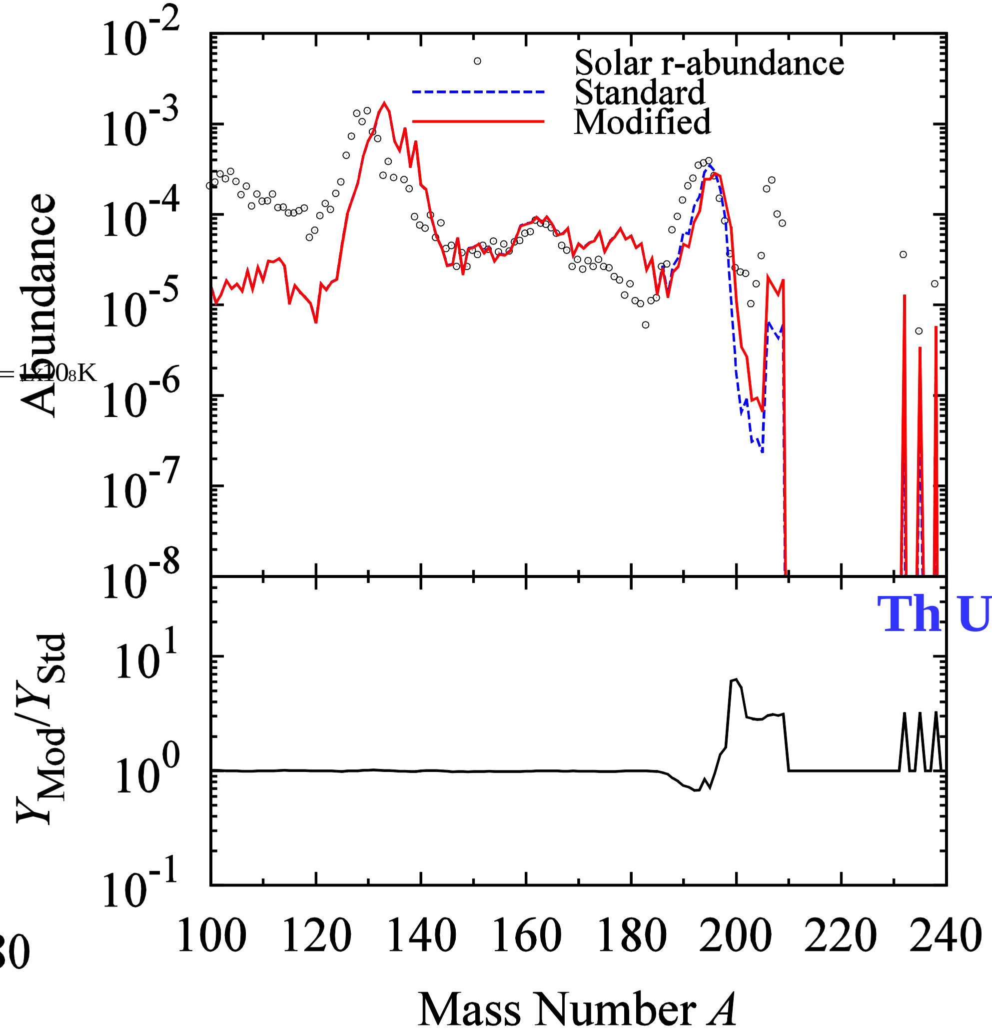

Summary

- **New ν –induced cross sections based on new shell-model Hamiltonians (SFO for p-shell, GXPF1 for pf-shell)**
- **Good reproduction of experimental data for $^{12}C\ (\nu, e^-)\ ^{12}N$, $^{12}C\ (\nu, \nu')\ ^{12}C$ and $^{56}Fe\ (\nu, e^-)\ ^{56}Co$**
- **(Effects of ν-oscillations in nucleosynthesis abundance ratio of $^{7}Li/^{11}B$ → ν mass hierarchy)**

- **GXPF1J well describes the GT strengths in Ni isotopes : ^{56}Ni two-peak structure confirmed by recent exp.**

→ ▪Accurate evaluation of e-capture rates at stellar environments
Nucleosynthesis in Type-I SNe; $^{58}Ni/^{56}Ni$ reduced

- **Detailed e-capture and beta-decay rates for URCA nuclear pairs in 8-10 solar-mass stars**

→ URCA density for A=25 and 23 with fine mesh of density and temperature

→ Cooling of O-Ne-Mg core by nuclear URCA processes determines the fate of the stars.

- **Half-lives of N=126 isotones are evaluated by shell-model calculations with GT and FF contributions.**

→ Shorter half-lives than FRDM

r-process nucleosynthesis up to Th and U at SNe and neutron-star mergers

Collaborators

T. Otsuka[e], T. Kajino [a,b], M. Honma[c], T. Yoshida[d], H. Toki[g], K. Nomoto[h], S. Jones[i], R. Hirsci[i]

[a]National Astronomical Observatory of Japan
[b]Dep. Of Astronomy, Univ. of Tokyo
[c]University of Aizu
[d]YITP, Kyoto University
[e]CNS and Dept. of Physisc, Univ. of Tokyo
[g]RCNP, Osaka University
[h]WPI, the Univ. of Tokyo
[i]Keele University